Supplement of Atmos. Chem. Phys., 25, 15437–15451, 2025
https://doi.org/10.5194/acp-25-15437-2025-supplement

Atmospheric Chemistry and Physics
Open Access
EGU

Supplement of

Impact of stratospheric intrusion on near-surface ozone over the Sichuan Basin in China driven by terrain forcing of Tibetan Plateau

Zhuozhi Shu et al.

Correspondence to: Tianliang Zhao (tlzhao@nuist.edu.cn)

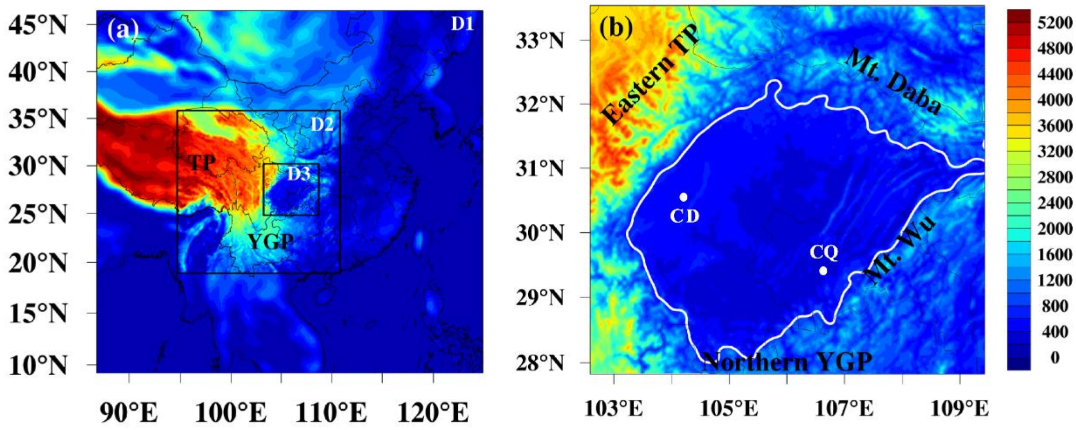

Fig S1. (a) WRF-Chem three nesting domains D1 (48 km), D2 (12 km) and D3 (3 km) with terrain heights (m; a.s.l.), (b) the finest-grid D3 surrounded by eastern TP (Tibetan Plateau), northern YGP (Yunnan-Guizhou Plateau), Mt. Wu (Mountain Wu) and Mt. Daba (Mountain Daba) with the location of Chengdu (CD) and Chongqing (CQ) cities. The SCB region is roughly outlined with white lines.

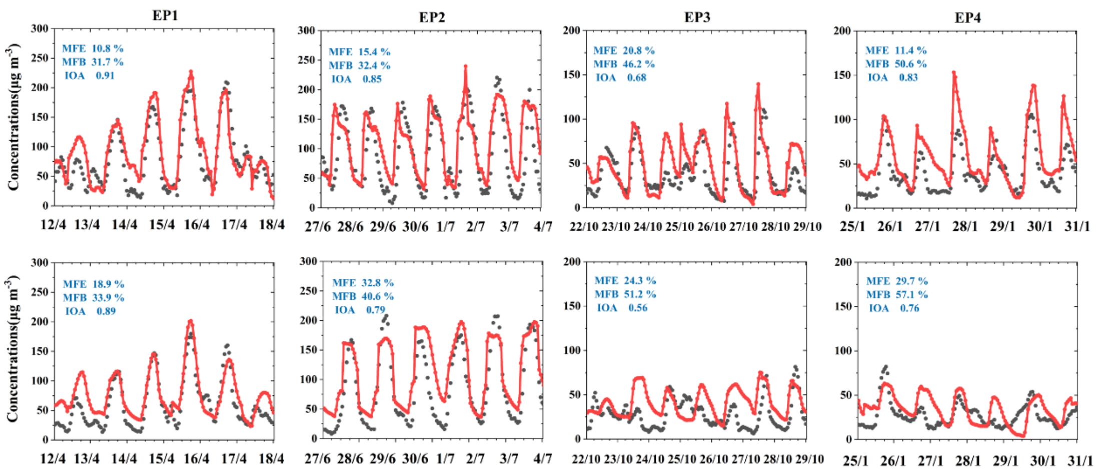

Fig S2. Comparisons of observed (gray points) and simulated (red curve) surface O_3 concentrations respectively at Chengdu (upper panels) and Chongqing (lower panels) with the statistics metrics. IOA, MFB and MFE were calculated as follows: IOA$=1-\frac{\sum_{i=1}^{N}(O_i-M_i)^2}{\sum_{i=1}^{N}(|M_i-\bar{O}|+|O_i-\bar{O}|)^2}$; $MFB=\frac{1}{N}\sum_{i=1}^{N}(2\cdot\frac{M_i-O_i}{M_i+O_i})\cdot 100\%$; $MFE=\sum_{i=1}^{N}\left|2\cdot\frac{M_i-O_i}{M_i+O_i}\right|\cdot 100\%$ (M and O respectively represented the results from simulation and observation).

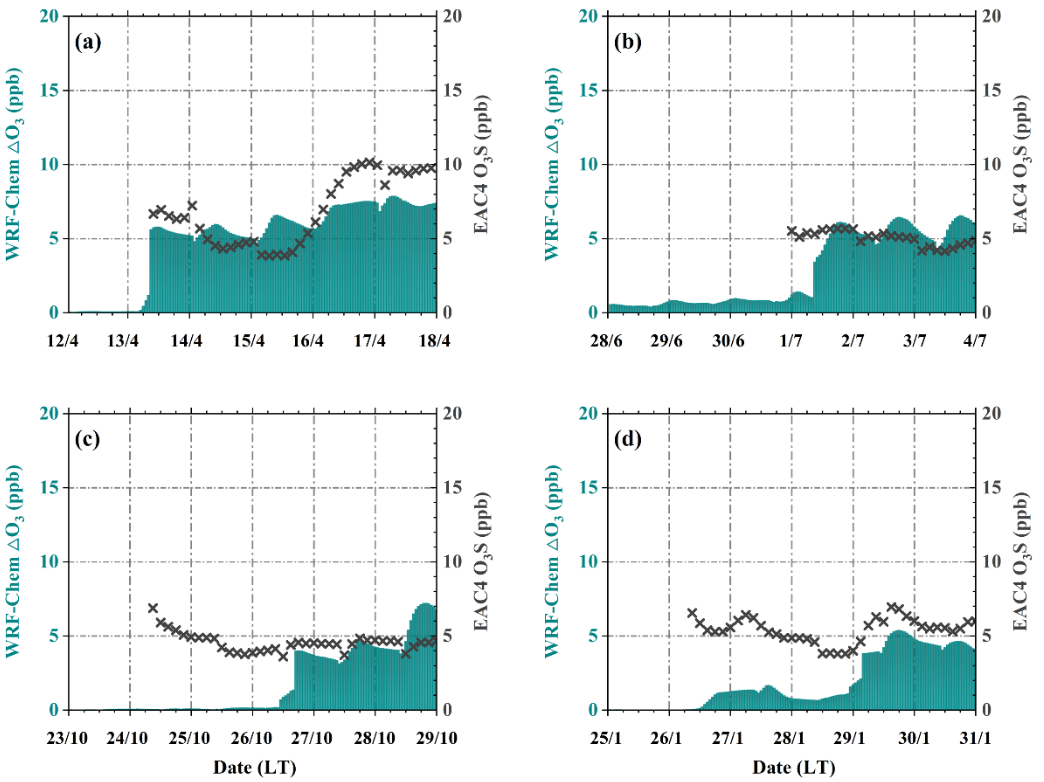

Fig S3. Comparison between hourly WRF-Chem △O_3 (ppb) and 3-hourly EAC4 O_3S (ppb) during the period of SI events (a) EP1, (b) EP2, (c) EP3 and (d) EP4 averaged over the SCB.

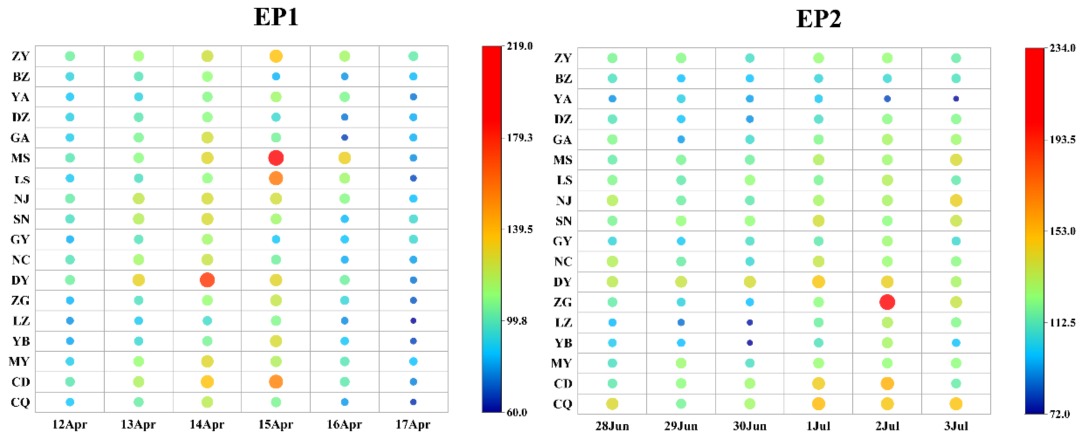

Fig S4. Daily maximum 8-hr average O_3 concentrations (μg m^{-3}) in 18 cities of SCB during EP1 and EP2.

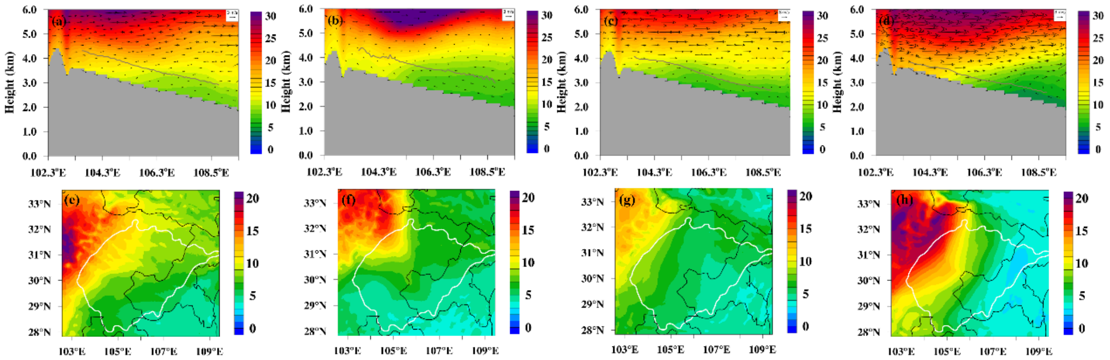

Fig S5. Height-longitude cross-sections of △O_3basin (ppb, color contours) and wind vectors averaged between 28–33 °N (upper panel), and spatial distribution of near-surface △O_3basin (ppb, color contours) (lower panel) during SI events of EP1 (a,e), EP2 (b,f), EP3 (c,g) and EP4 (d,h). The gray lines indicate atmospheric boundary layer height over the SCB and thick white lines roughly outline the SCB region.

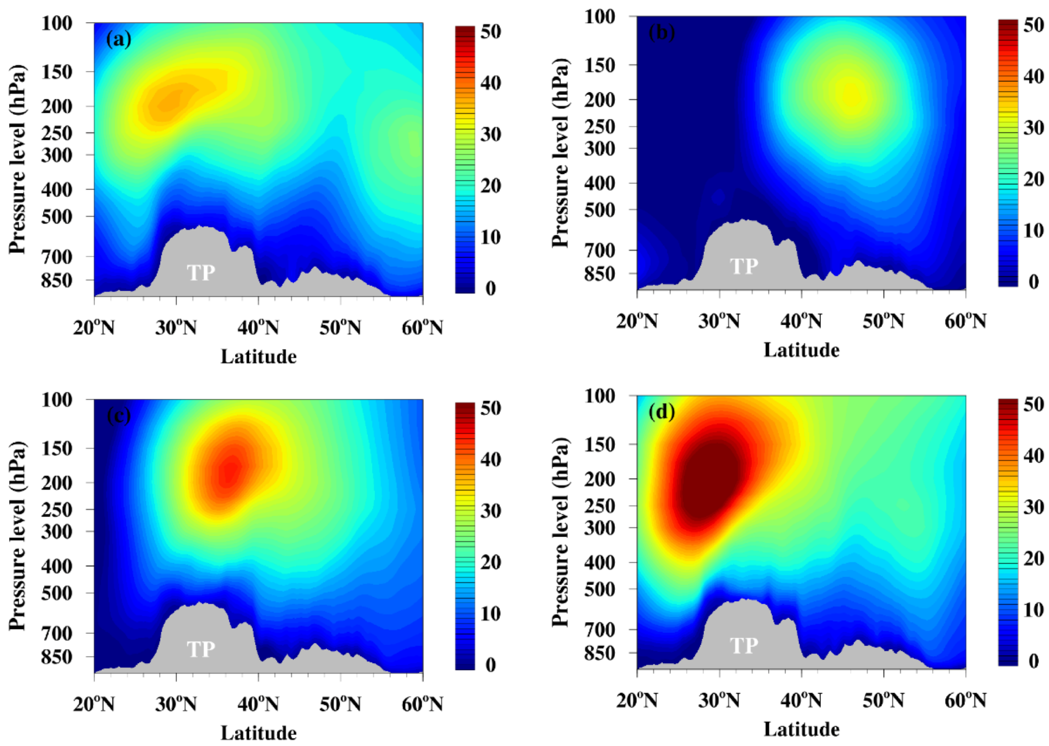

Fig. S6. Height-latitude cross-sections of monthly U wind speed (m s^{-1}) over the TP region, respectively in (a) April, (b) July, (c) October and (d) January of 2017.

Table S1. Setting of physical and chemistry schemes in the WRF-Chem simulations

Microphysics	Morrison 2-mom
Boundary layer	MYJ
Longwave radiation	RRTM
Shortwave radiation	RRTMG
Land surface	Noah
Cumulus convection	Grell 3D (none in D3)
Chemistry	RADM2
Aerosol particles	MADE/SORGAM
Photolysis	Madronich (TUV)
Dry deposition	Wesely

Table S2. The observed (Obs.) and simulated (Sim.) 2-m air temperature (T2), 10-m wind speed (WS10) and near-surface relative humidity (RH) averaged over 18 SCB with the statistical metrics during January, April, July and October in 2017 originated from Shu et al. (2023).

Variables	Obs.	Sim.	MB	ME	RMSE
T2	18.29 (°C)	18.68 (°C)	0.39	3.89	4.82
WS10	1.44 (m s^{-1})	1.95 (m s^{-1})	0.51	1.08	1.36
RH	77.39 (%)	72.31 (%)	-5.07	18.30	22.53

Note: MB, ME and RMSE were calculated as follows: $MB = \frac{1}{N}\sum_{i=1}^{N}(M_i - O_i)$; $ME = \frac{1}{N}\sum_{i=1}^{N}|M_i - O_i|$; $RMSE = \sqrt{\frac{1}{N}\sum_{i=1}^{N}(M_i - O_i)^2}$ (M and O respectively represented the results from simulation and observation).